Journal of Cleaner Production 278 (2021) 123477

Contents lists available at ScienceDirect

Journal of Cleaner Production

journal homepage: www.elsevier.com/locate/jclepro

Review

A corona-electrostatic technology for zinc and brass recovery from the coarse fraction of the recycling process of spent alkaline and zinc–carbon batteries

Laur Calin*, Andrei Catinean, Mihai Bilici, Adrian Samuila

Department of Electrotechnics and Measurements, Technical University of Cluj-Napoca, Romania

ARTICLE INFO

Article history:
Received 20 December 2019
Received in revised form
3 July 2020
Accepted 26 July 2020
Available online 4 August 2020

Handling editor: Yutao Wang

Keywords:
Spent alkaline and zinc-carbon batteries
Zinc and brass recovery
Free fall corona-electrostatic separation

ABSTRACT

The recycling of spent alkaline and zinc-carbon batteries aims to minimize the waste, to avoid environmental pollution, and to provide valuable secondary raw materials. The paper presents the development of a new technology, based on corona-electrostatic separation, for the recovery of zinc and brass granules from the coarse fraction obtained in the recycling process of alkaline and zinc-carbon batteries. A free-fall electrostatic separator was equipped with an extended needle-type corona electrode, to strongly charge by ion bombardment all the components of the granular mixture. The difference in density between metallic granules (zinc and brass) and other non-metallic components leads to different trajectories and makes possible their collection as separated fractions. The recovery rate and purity of the metallic fraction - as high as 99% and 92% respectively, was obtained with a 52% recovery rate the non-metallic fraction. A new electrode configuration was employed to improve the granule collection efficiency, leading to a significant increase in both the recovery rate of non-metallic fraction, and the purity of the metallic fraction - 97.6% and 99.2% respectively. The experimental results show that the proposed corona-electrostatic technology allows the recovery of about 390 kg of zinc and brass with over 99% purity from 1,000 kg of granular mixture, with an energy consumption of about 48 kWh. The corona-electrostatic technology represents a competitive alternative for the recovery of zinc and brass granules from spent alkaline and zinc-carbon batteries.

Contents

1. Introduction

Alkaline and zinc–carbon (Zn-C) batteries are single use

* Corresponding author.
E-mail address: Laurflorentincalin@yahoo.com (L. Calin).

https://doi.org/10.1016/j.jclepro.2020.123477
0959-6526/

portable batteries (primary cells) powering radios, remote controls, alarm clocks, MP3/CD players, digital cameras, etc. According to "European Portable Battery Association" (2017) around 225,000 t (11 × 10^9 units) portable (single use and rechargeable) batteries have been placed on the market in the EU in 2016, (52% alkaline and 12% zinc-carbon) with a collection rate of 44% (98,000 t). Seventeen countries have reached or exceeded a collection rate of 45% in 2016. With only 26%, Romania has the smallest collection rate ("European Portable Battery Association", 2017), while the EU legislation on waste batteries and accumulators stipulates that the member states must collect at least 45% and recycle 50% by average weight of waste batteries (Directive, 2006/66/EC, 2016). European regulations also emphasize that research and development of new environmentally friendly and cost-effective recycling technologies should be encouraged.

Batteries contain hazardous, toxic, and corrosive materials and if they end up in landfills the chemicals cause soil contamination and water pollution. The incineration of batteries cause air pollution and battery waste can endanger wildlife and is potentially hazardous to human health.

In accordance with the European Union Directives 2006/66/EC and 2008/103/EC, after 2008 the placing on the market of the batteries containing more than 0.0005% mercury and 0.002% cadmium is prohibited. Consequently, spent alkaline and Zn-C batteries, who continue to dominate the market, are no longer classified as hazardous waste, but the EU legislation prohibits the landfilling or the incineration of all type of batteries. The recycling of spent batteries is mandatory (European Union Directives, 2006/66/EC), aiming to minimize the waste and to avoid environmental pollution. Recycling of spent alkaline and Zn-C batteries preserve primary raw materials providing valuable secondary raw materials, specifically zinc (Zn) and manganese (Mn), at less energy consumption and lower production costs in comparison with the mining industry (Ekberg and Petranikova, 2018).

All the recycling processes of spent batteries contains some typical operations such as sorting, dismantling/shredding, and sieving (Fig. 1). The main purpose is to separate the fine fraction ("black mass") which is about 57% of the batteries total weight (Ferella et al., 2008) and contains about 33% Mn and 29% Zn (Ebin et al., 2016). This product represents the main source for recovered Zn and Mn from spent batteries (Espinosa and Mansur, 2019) by pyrometallurgical methods using: carbothermic reduction process (Yesiltepe et al., 2019), thermal transformation under argon atmosphere (Farzana et al., 2018) and hydrometallurgical processes using: acidic and alkaline mediums (Abid Charef, 2017), reducing agent with H_2S0_4 and H_2O_2 (Buzatu et al., 2004), H_2SO_4 and selective precipitation by NaOH at different pH (Chen et al., 2017), microwave assisted leaching method (Lanoo et al., 2019), treatment of the battery leachates by a ionic liquid diluted in toluene (Mahandra et al., 2018), reductive acid leaching ($H_2SO_4 + C_2H_2O_4$) (Sobianowska-Turek et al., 2016), solvent extraction, electrodeposition and precipitation methods (Tanong et al., 2017).

After a magnetic separation aiming to recover ferrous metals, the coarse fraction obtained in the pre-treatment process of alkaline and Zn-C batteries contains Zn granules from the negative electrode of Zn-C batteries (Fig. 2a), brass granules from the current collector of alkaline batteries (Fig. 2b), plastics from gaskets and paper/non-woven fabric/plastic from separators between electrolyte and battery electrodes. Different methods are proposed for the recovery of nonferrous metals (zinc and brass) from the mixture with non-metallic granules: eddy current separation (Ferella et al., 2008), pneumatic separation (Ruffino et al., 2011), or gravity separation (Gasper et al., 2013). All these methods are feasible, but many factors including the size of the granules strongly influence their efficiency. Neither the literature nor the recyclers give any information about the stages of the technology, or the purity and recovery rate of the non-ferrous metallic fraction.

The aim of this work is to propose a new and highly efficient method for the recovery of zinc and brass granules from this coarse fraction, using the corona-electrostatic separation technology.

This clean technology, characterized by zero waste and low energy consumption, is based on the difference in surface conductivity between the components of the granular mixture (Knoll and Taylor, 1985) and is well known as capable to separate conductive and non-conductive granules from waste electrical and electronic equipment (Samuila et al., 2005).

The rotating roll corona-electrostatic separator is the typical equipment in this technology, where the granules trajectories depend on their conductivity (Iuga et al., 2001). The granular mixture representing the coarse fraction in the recycling process of alkaline and Zn-C batteries contains non-ferrous metallic granules (zinc and brass) and non-conductive granules (plastic, paper and non-woven fabric), but all are covered by a fine powder of "black mass" characterized by high conductivity because of the graphite content. As a result, the trajectories of the two type of granules in the rotating roll corona-electrostatic separator are not differentiated.

This paper presents an innovative solution - a free-fall electrostatic separator equipped with a special corona electrode, to separate zinc and brass granules from other non-conductive components of the coarse fraction of the recycling process of alkaline and Zn-C batteries.

2. Materials and method

2.1. Materials

The coarse fraction that results in the recycling process of spent alkaline and Zn-C batteries is a mixture of zinc, brass, graphite, plastic materials, paper/cardboard, and non-woven fabrics (Fig. 3A). All the components of the fraction are covered in "black mass" powder that contains fine granules of Zn, MnO_2, KOH, NH_4Cl, $ZnCl_2$ and graphite and is characterized by high electrical conductivity.

In order to increase the efficiency of the free-fall corona-electrostatic separation the initial granular mixture was subjected to two preliminary operations. The first was a grinding operation aiming to dissociates the granule conglomerates, while the second was a pneumatic (zig-zag) separation that removed the light fraction, composed of black mass powder, lightweight plastic, paper/cardboard, and non-woven fabrics (Fig. 3C). This last operation has reduced the amount of material mixture for the corona-electrostatic separation by about 42% by weight but was not able to remove all the non-metallic granules. The heavy fraction (Fig. 3B) represents 58% of the initial material and contains zinc, brass, and larger/heavier plastic granules, all of them covered by the high conductivity black mass powder (Table 1).

3. Method

The separation of zinc and brass granules from the granular mixture obtained as heavy fraction (Fig. 3B) was achieved by an innovative solution - a free-fall electrostatic separator equipped with a special corona electrode that generates an extended corona charging zone (Fig. 4a). The granular mixture was introduced into the separator by means of an adjustable inclined plane and left to fall freely. In the corona discharge zone, all the granules get negative charge after being subjected to an intense ion bombardment.

The charge accumulated by the granules, especially plastic granules, in the corona discharge zone decisively influences their trajectories and consequently the separation results. For this reason, the efficiency of the charging process by ion bombardment

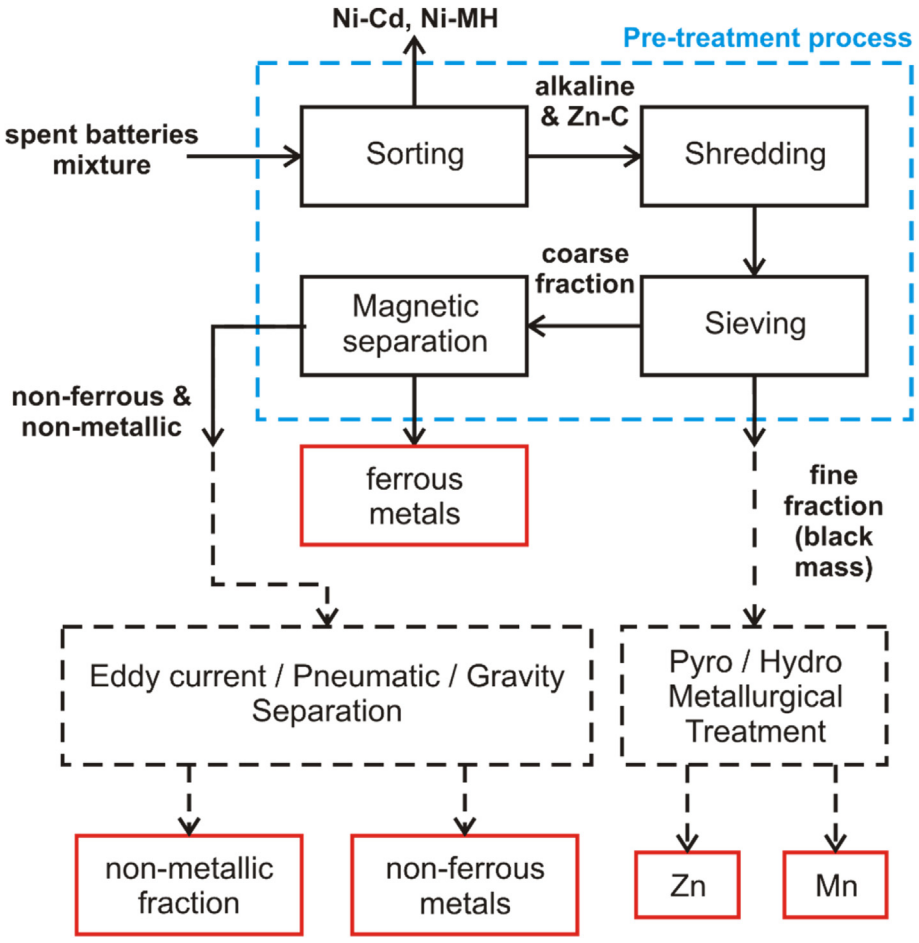

Fig. 1. Typical operation in the recycling process of the alkaline and Zn-C batteries.

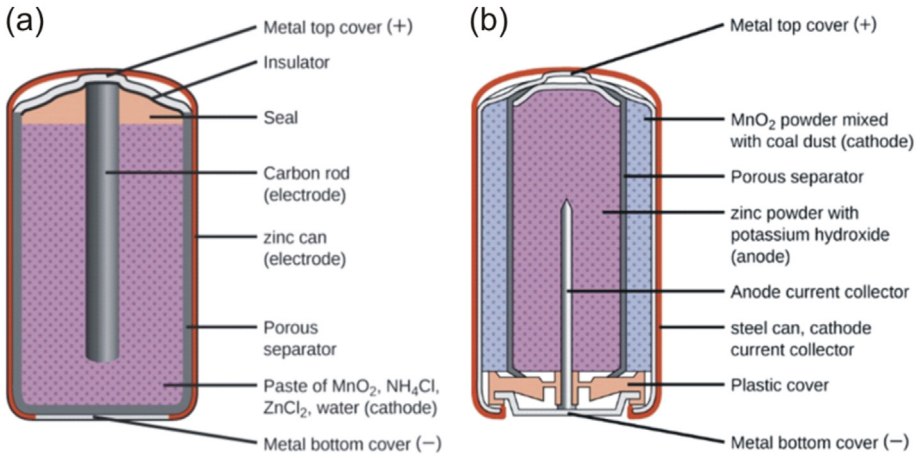

Fig. 2. Components of Zn-C (a) and alkaline (b) batteries (Chemistry, 2016).

is a key factor for a successful separation. In the case of our device, where the granules fall freely in the separation zone, an extended corona discharge zone is necessary to increase the granules' charge.

The granules entering the separator have an initial velocity v_0 and their trajectories in the electrostatic separation zone are primarily determined by the action of the gravity force F_G, the electrical force F_E exerted by the electric field, and the air drag force F_A (Fig. 4b):

$$F_G = mg \tag{1}$$

$$F_E = QE \tag{2}$$

$$F_A = \frac{1}{2} C_D \rho_A S v^2 \tag{3}$$

where m is the granule mass, g is the gravitational acceleration, E is

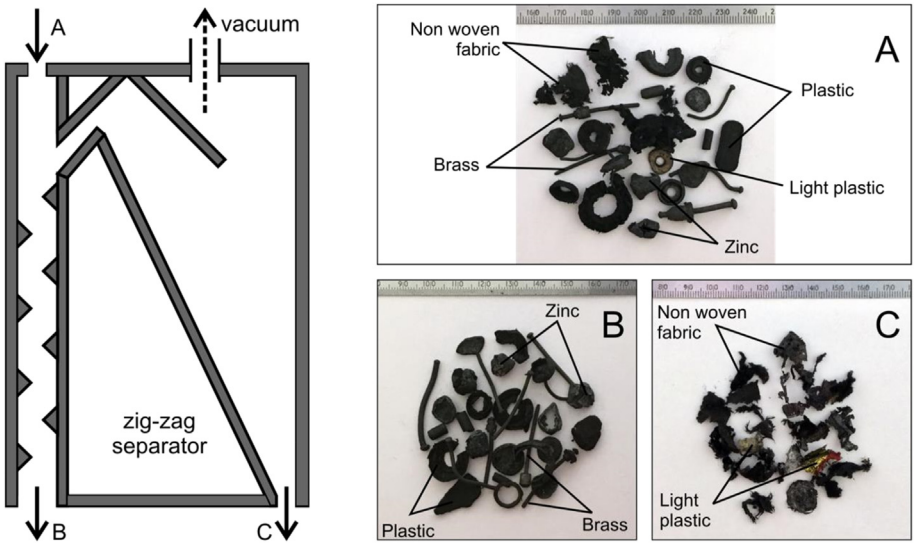

Fig. 3. Zig-zag separation principle, input material A, heavy fraction B, and light fraction C.

Table 1
Weight, density, shape, and size of the heavy fraction components.

Material	Average granule weight[a] (mg)	Volumetric mass density (kg/m^3)	Shape of granule	Size range (mm)	
				small	large
brass	394	8,610	cylinder	25 × 1	40 × 2
zinc	192	7,140	crumpled ball, pill	4 × 2	10 × 5
plastic	41	920	O-ring/flat pebble	4 × 5 x 1	18 × 5 x 1

[a] The average granule weight was calculated as the weight of 100 granules divided by 100.

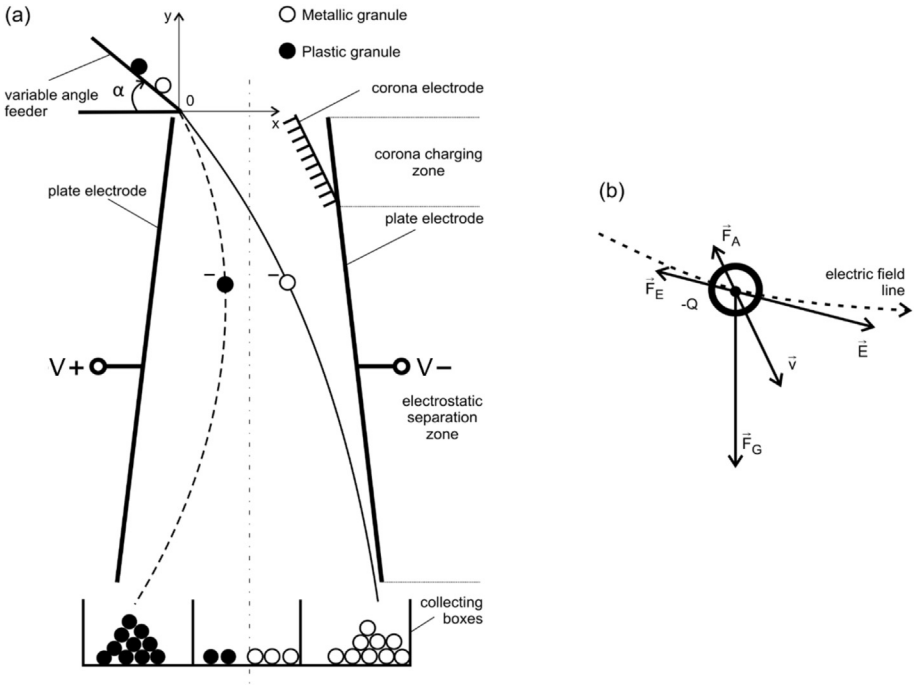

Fig. 4. The separation principle of metallic and plastic granules in the free-fall corona-electrostatic separator (a) and the forces that act on a granule in the electrostatic separation zone (b).

the electric field strength and Q is the electric charge acquired by the granule after being subjected to the ion bombardment, C_D is the drag coefficient, ρ_A is the air density, S is the particle projected surface on motion direction, and v is the particle velocity.

Due to the difference in the density between metallic and plastic granules, the displacement of the metallic granules is influenced predominantly by the gravity force F_G, while the electric field force F_E predominantly influenced the displacement of plastic granules. As a result, the separation trajectories of these two types of granules are different, which makes possible their collection as separated fractions.

The high voltage V of the electrodes (defined as the potential difference between the separator electrodes $V = |V+| + |V-|$) and the angle α of the granules inlet are the main parameters of the process influencing the separation results.

In order to optimize these parameters, the Design of Experiments (DoE) methodology was employed. Compared to the classical methodology, DoE has the following advantages: a considerable reduction of the number of experiments, the possibility of studying the effects of a large number of factors, detecting the interactions between factors, determining the results with a good accuracy and the assisted model of the results (Goupy and Creighton, 2007). The method consists in establishing an experience plan capable to generate a polynomial model which describes the dependence between the output function y (response) and the input variables u_i (factors), as follows:

$$y = f(x_i) = a_0 + \sum a_i x_i + \sum a_{i,j} x_i x_j + \sum a_{i,i} x_i^2 \quad (4)$$

where a_i are the coefficients of a quadratic polynomial model and x_i is the normalized centered value for each factor u_i:

$$x_i = \frac{(u_i - u_{i0})}{\Delta u_i} = u_i^* \quad (5)$$

with

$$u_{i0} = \frac{u_{i\max} + u_{i\min}}{2}; \Delta u_i = \frac{u_{i\max} - u_{i\min}}{2} \quad (6)$$

$$u_{i0} = \frac{u_{i\max} + u_{i\min}}{2}; \Delta u_i = \frac{u_{i\max} - u_{i\min}}{2} \quad (7)$$

The coefficients can be calculated using a specialized software - MODDE (Umetrics, Sweden), that assists the user for interpretation of the results and prediction of the responses and identifies best adjustments of the factors for optimizing the process.

Moreover, the program calculates two statistical criteria: the "goodness of fit": R^2, and the "goodness of prediction": Q^2. The latter is a measure of how well the model will predict the responses for new experimental conditions. A good mathematical model has criteria R^2 and Q^2 with the numerical value approaches unity and preferably not separated by more than 0.2–0.3 (MODDE, 1999).

Before the start of the experiments, it is necessary to set the best and suitable design that can model the process with the most possible precision. In this paper, the full factor (3 levels) design, requesting a total of 12 separation experiments (one in each point of the experimental matrix and 3 repetitions in the central point) was adopted (Fig. 5). The input parameters of the separation process (factors) were the voltage V and the angle α, while the output parameters (responses) were the recovery rate and purity for both metallic and plastic fractions.

The low and the high limit of the supply voltage V and of the inlet angle α was set as a result of a series of preliminary experiments, as follows: V_{min} = 80 kV, V_{max} = 88 kV and α_{min} = 27°, α_{max} = 31°, respectively.

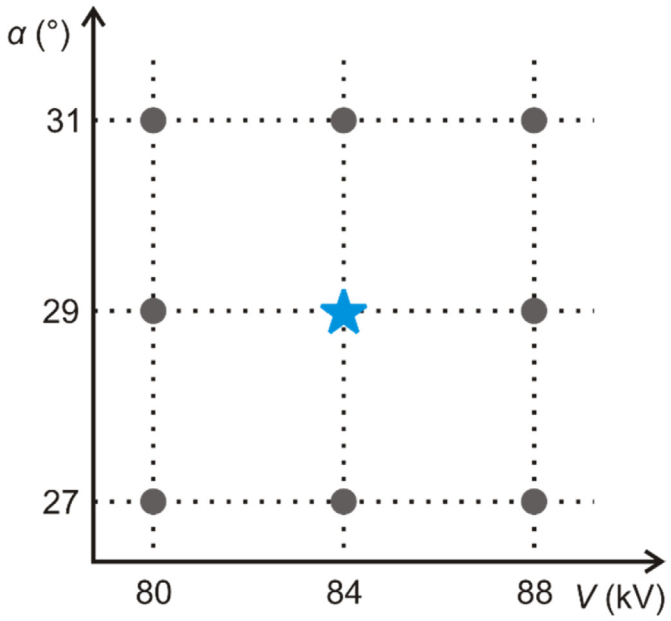

Fig. 5. Graphical representation of the experimental points of the full factors (3 levels) quadratic model with angle α and voltage V as input factors of the free-fall corona-electrostatic separation process.

For the factors considered in the present study, the quadratic model of the responses takes the following form:

$$y(\%) = a_0 + a_1 V^* + a_2 \alpha^* + a_{12} V^* \alpha^* * + a_{11} V^{*2} + a_{22} \alpha^{*2} \quad (8)$$

were V* and α* are the normalized centered value for each factor V and α, calculated using formulas (5) and (6).

4. Experimental device

Two novel types of electrodes able to generate the extended corona discharge zone in the free fall separator were designed and tested in the laboratory. The first electrode (Fig. 6a) is an assembly of 24 tungsten wires of 0.2 mm diameter and 200 mm length, fixed on a copper frame and set apart 20 mm from each other. The second electrode (Fig. 6b) is made as an array of 540 needles of 25 mm length and 0.8 mm diameter fixed at a distance of 10 mm from each another on a drilled 170 × 290 mm printed circuit board, connected through a copper layer of the PCB.

The *I-V* characteristics at three different gaps between the negative corona electrode and the positive plate electrode highlight higher discharge currents for the needle array electrode (Fig. 6c). Turn-on voltages and average current densities are higher for this type of electrode, while breakdown voltages are lower. For this reason, the needle array electrode was chosen to generate the extended corona discharge zone of the free fall separator, but the electrode gaps used were larger than 250 mm. This way, voltages between 80 and 88 kV can be used without getting air breakdown.

The separation experiments of zinc and brass granules from other non-metallic components (mainly plastics) of the heavy fraction were performed on a free-fall electrostatic separator (Fig. 7) equipped with the needle array type corona electrode. An extended corona discharge zone required to charge the granules by ion bombardment (Dascalescu et al., 1994) was generated by connecting the corona electrode to an adjustable high voltage supply (model Gamma RR100-3R) of negative polarity $V-$. The same high voltage supply was used for the negative polarity plate electrode

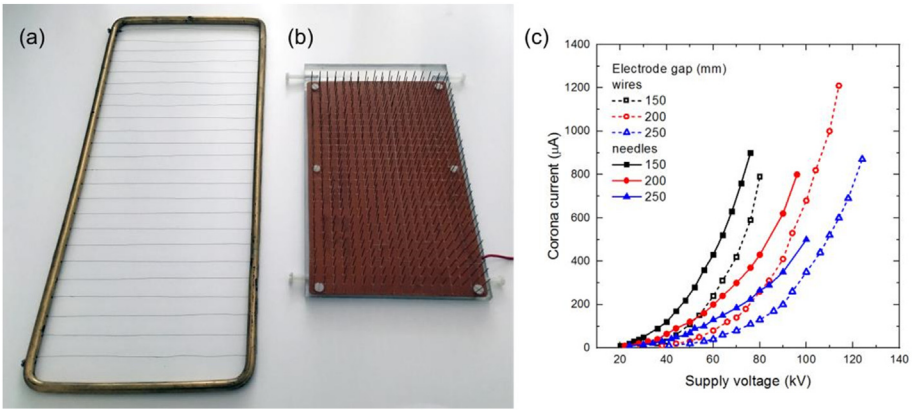

Fig. 6. Types of corona electrode designed and tested in the laboratory: parallel wires (a) and needle array (b), and corona discharge I-V curves for the electrodes at three different gaps (c).

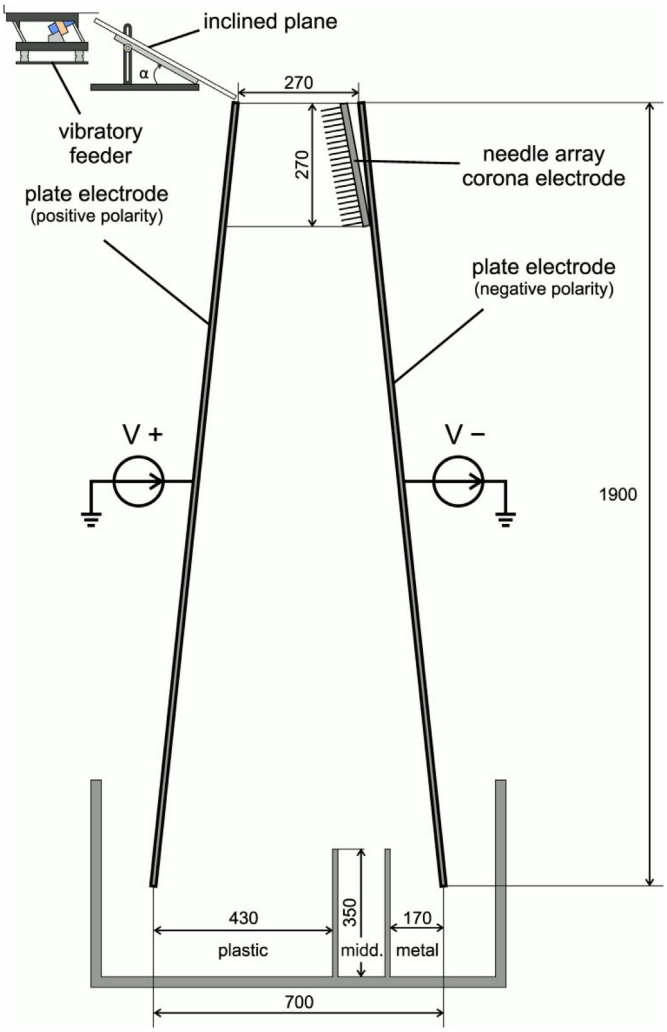

Fig. 7. Free fall corona-electrostatic separator equipped with an extended needle array corona electrode.

associated with the corona electrode. The other plate electrode of the free-fall separator was connected to a similar high voltage supply of positive polarity $V+$, so that the potential difference between the separator electrodes was $V = |V+| + |V-|$. The separator was equipped with three collecting boxes, one for the metal fraction, one for the plastic fraction, and another for the middling fraction, resulted from the electrostatic separation process. A vibratory feeder and an inclined plate were employed to introduce the granular material in the separation zone with a constant feed rate of 130 g/min. The angle α of the plate represents a very important parameter allowing to control the granules trajectories and consequently the separation results.

5. Results and discussion

5.1. Experimental results

A series of 12 corona-electrostatic separation experiments was carried out on the free fall corona-electrostatic separator with parameters set according to the DoE full factor (3 levels) quadratic plan (Fig. 5). A large quantity was used for each sample (800 g) in order to reduce the errors due to granular material non-homogeneity. The content analysis of the three separation fractions for each run allowed the calculation of the recovery rate and purity for both metallic and plastic fractions (Table 2). The separation indicators were calculated as follows: *recovery rate* = ratio of the recovered material weight to material weight in sample, and *purity* = ratio of the recovered material weight to separated fraction weight. The purity of the plastic fraction was virtually 100% for all 12 experiments and it was excluded from the table.

Processing the experimental results by the MODDE 5.0 software allowed to calculate the value of the coefficients of the polynomial model (8) and the uncertainty in their determination. The coefficients whose uncertainties were greater than their value are not statistically significant and were removed from the models. The contribution of each factor (V and α) on the responses (recovery and purity) is given by the values of the corresponding coefficients in the following mathematical models:

$$Metal\ recovery(\%) = 96.87 + 3.47\alpha^* \quad (9)$$

$$Metal\ purity(\%) = 90.67 + 1.37V^* - 2.24\alpha^* + 1.02V^*\alpha^* + 1.33\alpha^{*2} \quad (10)$$

$$Plastic\ recovery(\%) = 48.54 + 5.51V^* - 7.29\alpha^* + 2.5\alpha^{*2} \quad (11)$$

The polynomial expressions for metal recovery rate (9) and purity (10) are validated by the excellent values of the diagnostic parameters $R^2 = 0.968$, $Q^2 = 0.908$ and, $R^2 = 0.999$, $Q^2 = 0.967$

Table 2
Results of 12 separation runs on the free-fall corona-electrostatic separator as part of a design of experiments quadratic model where voltage and input angle α were factors and metal purity, metal recovery rate, and plastic recovery rate were responses.

Run number	Voltage V (kV)	Input angle α (°)	Metal recovery rate (%)	Metal purity (%)	Plastic recovery rate (%)
1	80	27	94.78	93.71	55.76
2	84	27	92.01	94.2	58.1
3	88	27	93.48	95.06	60.2
4	80	29	98.38	88.96	43.07
5	84	29	97.7	90.71	49.02
6	88	29	98.26	91.15	51.34
7	80	31	99.05	87.19	37.56
8	84	31	98.96	89.72	43.51
9	88	31	99.08	91.93	51.86
10	84	29	96.02	90.75	48.74
11	84	29	93.7	94.39	55.82
12	84	29	93.65	95.82	59.48

respectively. It indicates that the most important factor is the angle α.

In order to obtain a high metal recovery rate, the angle α must be increased, and for a greater metallic fraction purity, the angle α must be decreased. The mathematical model of the plastic recovery rate has the "goodness of fit" and "goodness of prediction" values $R^2 = 0.996$ and $Q^2 = 0.855$, respectively. It shows that both factors have an important effect: high voltage and low angle lead to an increased recovery rate of plastic fraction.

The combined effects of the two factors is highlighted by the response surfaces, represented as contour plots in Fig. 8.

The response surfaces show that the angle α is the decisive factor for the recovery rate of the metallic fraction. Higher input velocity of the granules is obtained at $\alpha = 31°$ and, as the metallic granules displacement towards the positive electrode is less influenced by the electric force F_E, they are almost completely collected in the collecting box reserved for the metallic fraction (Fig. 8a). The supplied voltage, or in other words, the space charge density generated by the corona discharge and the amount of charge accumulated by the metallic granules by ion bombardment do not significantly influence their trajectories because the electric field force F_E has an order of magnitude lower (amounting to about 4–5%) than the gravity force F_G (Table 3). At lower angles the input velocity decreases, the granules are submitted to the ion bombardment for a longer time, and accumulate a larger amount of charge, so that their trajectories are more influenced by the electric field force F_E. Therefore, more zinc and brass granules are collected as middling, even more so as the supply voltage V (the electric field strength E) is higher. Even under these conditions, metallic granules do not contaminate the plastic fraction, which explains the 100% purity of the plastic fraction in all 12 separation runs.

The highest recovery rate of the plastic fraction is obtained at the lowest angle α and the maximum supply voltage V. In this case the input velocity of the granules is low, the charge accumulated by the plastic granules consequently increases and, at high voltages, they are strongly deviated by the F_E force (representing 20% of the gravity force, as shown in Table 3) towards the positive electrode, leading to an increased recovery rate (Fig. 8c). At higher input angles the input velocity of the granules increases, the charge acquired by the plastic granules by ion bombardment decreases, and many of them get collected as middling or end up with the metallic fraction, leading to a decrease in the recovery rate of the plastic fraction.

Using the "Optimizer" function of MODDE, it was possible to determine the values of the two factors that maximize the recovery and purity of the metal and plastic. At $V = 88$ kV and $\alpha = 31°$ the predicted metal purity and recovery rate are 91.93% and 99.08%

Table 3
Charge/mass ratio Q/m experimentally determined from samples of 100 g for each material, single granule charge Q, gravity force F_G, electric field force F_E and F_E/F_G ratio.

Material	Brass	Zinc	Plastic
Charge/mass ratio Q/m (nC/g)	−2.35	−2.87	−11.34
Single granule average charge Q (nC)	−0.93	−0.55	−0.46
$F_G = mg$ (mN)	3.86	1.88	0.40
$F_E = QE$[a] (mN)	0.16	0.09	0.08
F_E/F_G	0.04	0.05	0.2

[a] The electric field strength was calculated as $E = V/d = 1.68 \cdot 10^5$ V/m (V = 84 kV, d = 500 mm).

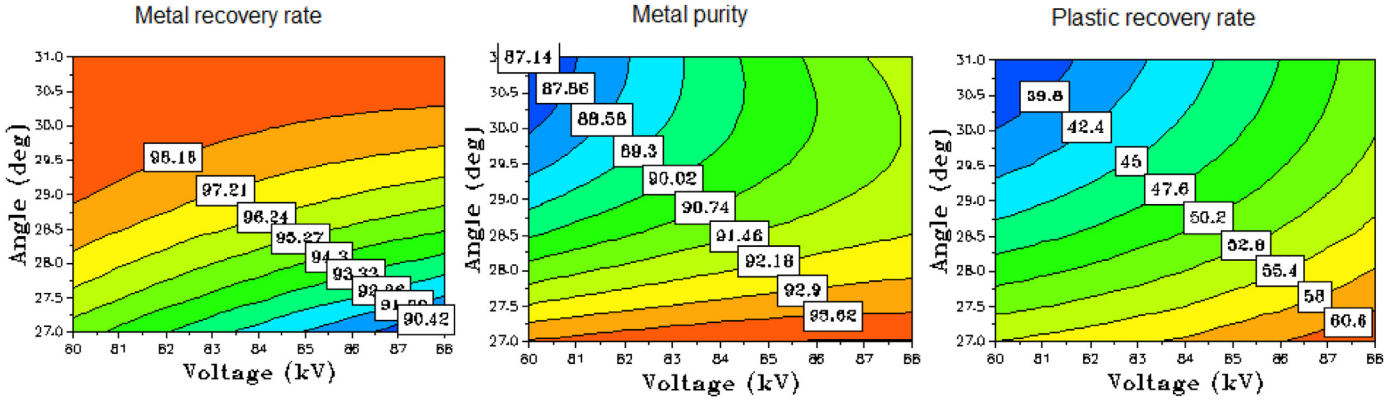

Fig. 8. Predicted contour plots for the recovery rate of metal (a) and plastic (b) fractions, as well as the purity of the metallic fraction (c).

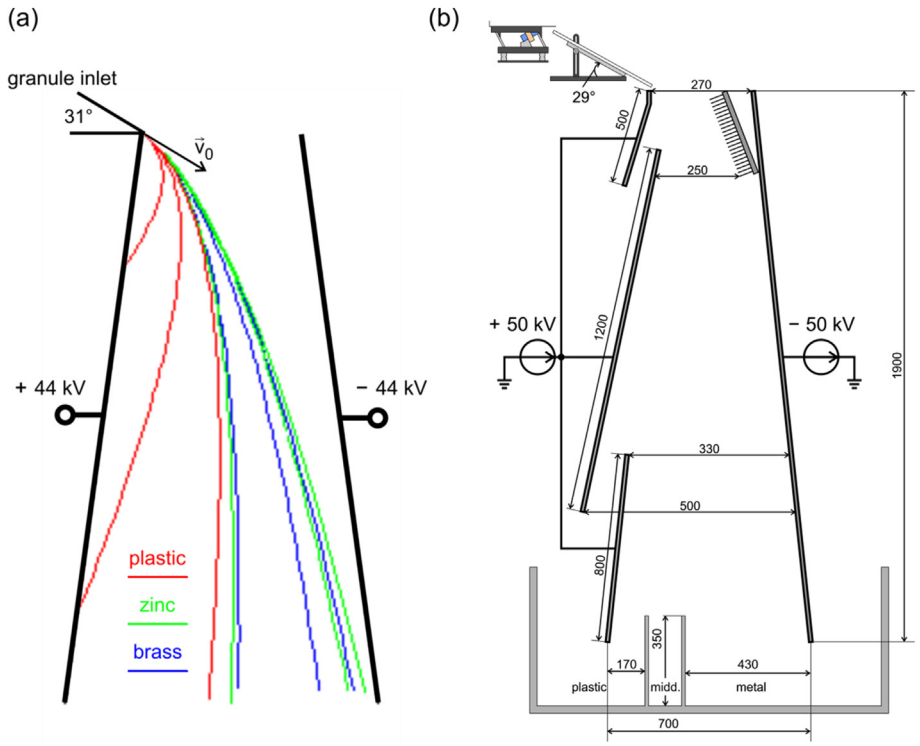

Fig. 9. Matlab simulation of plastic and metal (zinc and brass) granules trajectories for small, medium and large size granules (a) and the new electrode configuration of the free-fall corona-electrostatic separator (b).

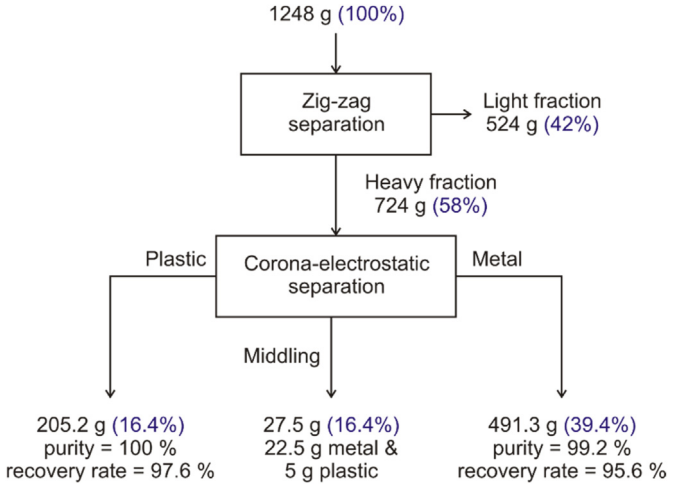

Fig. 10. Separation flow sheet for the new electrode configuration.

respectively, and the plastic recovery rate is 51.86%.

The purity of the metallic fraction is closely related to the recovery rate of the plastic fraction (Fig. 8b). At high voltage values and low angle values the plastic granules acquire a larger amount of charge, thus being strongly deviated by the electric field force F_E towards the positive electrode and are collected in their reserved collecting box without contaminating the metallic fraction. In contrast, at low voltages and high angles the plastic granules' charge decreases and their trajectories are less deviated towards the positive electrode, so they can get collected with the metallic fraction, lowering its purity.

5.2. Results of the numerical simulation

The 2D numerical simulation of the trajectories of the metallic and plastic granules in the free fall corona-electrostatic separator was done using Matlab, based on equations that describe their movement under the action of the gravity force F_G, the electric field force F_E, and the air drag force F_A:

$$\begin{cases} d_x = v_{0x}\Delta t + \frac{1}{2}a_x\Delta t^2 \\ d_y = v_{0y}\Delta t + \frac{1}{2}a_y\Delta t^2 \end{cases} \quad (12)$$

$$\begin{cases} v_x = v_{0x} + a_{0x}\Delta t \\ v_y = v_{0y} + a_{0y}\Delta t \end{cases} \quad (13)$$

$$\begin{cases} a_x = \frac{1}{m}(qE_x + F_{Ax}) \\ a_y = \frac{1}{m}(mg + qE_y + F_{Ay}) \end{cases} \quad (14)$$

where the terms with x and y indexes represent the projections in a cartesian $x0y$ system (Fig. 4) of the field strength E, the drag force F_A, the displacement d, velocity v, and acceleration a of a single granule. The charge acquired by the granules by ion bombardment in the corona charging zone was experimentally measured using a Faraday pail connected to a Keithley 6514 electrometer. The voltage drop between the electrodes was set at 88 kV and the inlet angle at 31°. Four runs were performed for each sample, then the average charge/mass ratio Q/m was calculated as shown in Table 3. The single granule average charge was calculated as Q/m multiplied by the granule average weight from Table 1 and this charge was further used in the numerical simulation of the granule trajectories.

Table 4
Corona - electrostatic treatment of 1,000 kg of granular material. Assessment of the energy consumption based on laboratory experiments.

Operation	Grinding (crushing)	Zig-zag separation (pneumatic)	Feeding (vibratory feeder)	Free-fall separation
Energy consumption (kWh)	20	20	4	4
Total (kWh)	48			

The gravity force F_G and the electric field force F_E were also calculated for a single granule in order to compare the ratio F_E/F_G for the three granule types.

The results shown in Table 3 explain the different behaviour of metallic and plastic granules in the electrostatic field zone of the free-fall separator. After the granules leave the corona discharge zone their trajectories are primarily influenced by the forces F_G and F_E (Fig. 4). The ratio F_E/F_G is of low value for zinc and brass granules and (4–5) times greater for plastic granules, allowing their collection as separated fractions.

The results of the numerical simulation (Fig. 9a) confirm the feasibility of the corona-electrostatic separation on the free-fall separator of the granular mixture composed of metallic and plastic granules originating from spent batteries. In the case of plastic granules, the higher ratio F_E/F_G shows that their trajectories are heavily influenced by the electric field force, directly dependent on the charge acquired in the corona discharge zone. On the contrary, the F_E force has a much lower influence on the of the metallic granule trajectories for which the ratio F_E/F_G has a very low value.

On the other hand, the experimental observations are confirmed - the lightweight plastic granules collide with the positive electrode and are diverted to the metallic fraction box, which leads to a decrease in the recovery rate of the plastic fraction and the purity of the metallic fraction. For this reason, it was decided to use a new, reconfigured, positive electrode, in order to allow the collecting of plastic granules by avoiding their collision with the electrode (Fig. 9b).

The results of the separation test carried out with the new electrode configuration show a significant increase of the recovery rate of the plastic granules without diminishing the purity of this fraction (Fig. 10). For this reason, the new electrode configuration also leads to an increase of the metallic fraction purity.

The experimental results presented in Fig. 10 show a 39% by weight metal content of the granular mixture originating from the recycling process of the alkaline and Zn-C batteries. The valuable non-ferrous metals, namely zinc and brass, from the spent batteries can be separated using the free-fall corona-electrostatic technology with 95.6% recovery rate and 99.2% purity.

The corona-electrostatic separation is a “zero waste” process because the middling fraction is fed a second time through the separator. Considering the small amount of plastic in this fraction, in an industrial process this product could be mixed with the metallic fraction, this way increasing the metal recovery rate to 100%.

The free-fall corona-electrostatic separation represents a real alternative to other technologies for the recovery of zinc and brass granules from the coarse fraction obtained in the recycling process of alkaline and zinc-carbon batteries. This clean and environmentally friendly technology leads to high purity and high recovery rate of the non-ferrous metallic fraction. Furthermore, this technology is characterized by low energy consumption (Table 4), contributing to a cost-effective recycling process. In this proposed technology the most important energy consumers are the grinding process and the pneumatic separation. To increase the recycling process profitability even more, further experimental research should be done in finding an operation mode of the free-fall corona-electrostatic separator allowing it to run without the crushing and pneumatic separation stages. Additionally, further experiments must be performed with different material samples, to assess the robustness of this technology.

6. Conclusions

The corona-electrostatic technology represents a competitive alternative for the recovery of zinc and brass granules from the coarse fraction obtained in the recycling process of alkaline and Zn-C batteries. This simple and environmentally friendly technology is characterized by zero waste and low energy consumption, that facilitates the profitability of the recycling process.

Some innovative solutions have been employed, for example the free-fall separator was equipped with a corona electrode. Another special corona electrode was developed to generate an extended space charge electric field zone. Additionally, a new configuration of the positive electrode was used to facilitate the collection of plastic granules thus avoiding their collision with the electrode. In the proposed technology a new parameter was introduced, the inlet angle α which has a decisive influence on the separation process, improving the separation results.

Recovery rate and purity of the metallic fraction as high as 99% and 92% respectively, were obtained at 88 kV high voltage level and 31° inlet angle, with about 52% non-metallic fraction recovery rate. A new electrode configuration was employed to improve the granule collection efficiency, leading to a significant increase in both the recovery rate of non-metallic fraction and purity of the metallic fraction, 97.6% and 99.2%, respectively. The purity of the plastic fraction was virtually 100%.

The experimental results presented in this paper show that the free-fall corona-electrostatic separation technology allows the recovery of about 390 kg of zinc and brass with over 99% purity, from 1,000 kg of granular mixture obtained as coarse fraction in the recycling process of spent alkaline and zinc-carbon batteries, with “zero waste” and an energy consumption of about 48 kWh.

In view of industrial application, further experimental research should be done to find an operation mode of the free-fall electrostatic separator allowing to simplify the process, giving up the crushing and pneumatic separation stage and increasing the recycling process profitability. Also, the robustness of the technology must be assessed by further experiments performed with different material samples.

Declaration of competing interest

The authors declare that they have no known competing financial interests or personal relationships that could have appeared to influence the work reported in this paper.

Acknowledgements

This work was supported within the research program “PN-III-P1-1.2-PCCDI-2017-0652, project NR. 84PCCDI - March 01, 2018 TRADE-IT. The authors would like to acknowledge with thanks their colleagues Petru Costel for his contribution to the development of the experimental equipment and Erasmus students Cloe Valenti and Nathan Courtois for their involvement in the experimental work.

References

Abid Charef, S., Affoune, A., Caballero, S., Cruz-Yusta, M., Morales, J., 2017. Simultaneous recovery of Zn and Mn from used batteries in acidic and alkaline mediums: a comparative study. Waste Manag. 68, 518–526. https://doi.org/10.1016/j.wasman.2017.06.048.

Buzatu, T., Buzatu, M., Saceanu, M., Petrescu, M., Ghica, G., 2014. Recovery of zinc and manganese from spent batteries by reductive leaching in acidic media. J. Power Sources 247, 612–617. https://doi.org/10.1016/j.jpowsour.2013.09.001.

Chemistry, 2016. Chapter 17. Electrochemistry, 17.5 batteries and fuel cells. Primary batteries. https://opentextbc.ca/chemistry/chapter/17-5-batteries-and-fuel-cells/ (accessed 02 April 2020).

Chen, W.-S., Liao, C.-T., Lin, K.-Y., 2017. Recovery zinc and manganese from spent battery powder by hydrometallurgical route. Enrgy. Proced. 107, 167–174. https://doi.org/10.1016/j.egypro.2016.12.162.

Dascalescu, L., Morar, R., Iuga, A., Samuila, A., Neamtu, V., Suarasan, I., 1994. Charging of particulates in the corona field of roll-type electroseparators. J. Phys. D Appl. Phys. 27, 1242–1251. https://doi.org/10.1088/0022-3727/27/6/023.

Directive 2006/66/EC on batteries and accumulators and waste batteries and accumulators as regards placing batteries and accumulators on the market https://eur-lex.europa.eu/legalcontent/EN/TXT/PDF/?uri=CELEX:32008L0103&from=GA (accessed 10 November 2019).

Ebin, B., Petranikova, M., Steenari, B.-M., Ekberg, C., 2016. Effects of gas flow rate on zinc recovery rate and particle properties by pyrolysis of alkaline and zinc-carbon battery waste. J. Anal. Appl. Pyrol. 121, 333–341. https://doi.org/10.1016/j.jaap.2016.08.014.

Ekberg, C., Petranikova, M., 2018. Recycling of Spent Batteries. Royal Swedish Academy of Engineering Sciences. https://www.iva.se/globalassets/presentationer-fran-seminarier/ekberg–iva-20180112—framtidens-batterier-id-114812.pdf (accessed 02 April 2020).

Espinosa, D., Mansur, M., 2019. Recycling batteries. In: Goodship, V., Stevels, A., Huisman, J. (Eds.), Waste Electric and Electronic Equipment (WEEE) Handbook, second ed. Woodhead Publishing Limited, Cambridge, pp. 371–391.

European Portable Battery Association (EPBA), 2017. The Collection of Waste Portable Batteries in Europe in View of the Achievability of the Collection Targets Set by Batteries Directive 2006/66/EC. August 2013, update December 2017. https://www.epbaeurope.net/resources/reports/ (accessed 10 November 2019).

Farzana, R., Rajarao, R., Hassan, K., Behera, P.R., Sahajwalla, V., 2018. Thermal nanosizing: novel route to synthesize manganese oxide and zinc oxide nanoparticles simultaneously from spent Zn-C battery. J. Clean. Prod. 496, 478–488. https://doi.org/10.1016/j.jclepro.2018.06.055.

Ferella, F., De Michelis, I., Veglio, F., 2008. Process for the recycling of alkaline and zinc–carbon spent batteries. J. Power Sources 183, 805–811. https://doi.org/10.1016/j.jpowsour.2008.05.043.

Gasper, P., Hines, J., Miralda, J.-P., Bonhomme, R., Schaufeld, J., Apelian, D., Wang, Y., 2013. Economic feasibility of a mechanical separation process for recycling alkaline batteries. J. New Mat. Electr. Sys. 16, 297–304. https://doi.org/10.14447/jnmes.v16i4.157.

Goupy, J., Creighton, L., 2007. Introduction to Design of Experiments with JMP Examples. SAS Institute, Cary, NC.

Iuga, A., Morar, R., Samuila, A., Dascalescu, L., 2001. Electrostatic separation of metals and plastics from granular industrial wastes. IEE Proc. Sci. Meas. Technol. 148, 47–54. https://doi.org/10.1049/ip-smt:20010356.

Knoll, F.S., Taylor, J.B., 1985. Advances in electrostatic separation. Min. Metall. Expl. 2, 106–114. https://doi.org/10.1007/BF03402605.

Lanoo, S., Vilas-Boas, A., Sadeghi, S.M., Jesus, J., Soares, H.M.V.M., 2019. An environmentally friendly closed loop process to recycle raw materials from spent alkaline batteries. J. Clean. Prod. 236, 117612. https://doi.org/10.1016/j.jclepro.2019.117612.

Mahandra, H., Singh, R., Gupta, B., 2018. Recycling of Zn-C and Ni-Cd spent batteries using Cyphos IL 104 via hydrometallurgical route. J. Clean. Prod. 172, 133–142. https://doi.org/10.1016/j.jclepro.2017.10.129.

ODDE 5.0 User Guide and Tutorial, 1999, Umetrics AB, Umea.

Ruffino, B., Zanetti, M., Marini, P., 2011. A mechanical pre-treatment process for the valorization of useful fractions from spent batteries. Resour. Conserv. Recycl. 55, 309–315. https://doi.org/10.1016/j.resconrec.2010.10.002.

Samuila, A., Urs, A., Iuga, A., Morar, R., Aman, F., Dascalescu, L., 2005. Optimization of corona electrode position in roll-type electrostatic separators. IEEE Trans. Ind. Appl. 41, 527–534. https://doi.org/10.1109/TIA.2005.844859.

Sobianowska-Turek, A., Szczepaniak, W., Maciejewski, P., Gawlik-Kobylińsk, M., 2016. Recovery of zinc and manganese, and other metals (Fe, Cu, Ni, Co, Cd, Cr, Na, K) from Zn-MnO2 and Zn-C waste batteries: hydroxyl and carbonate co-precipitation from solution after reducing acidic leaching with use of oxalic acid. J. Power Sources 325, 220–228. https://doi.org/10.1016/j.jpowsour.2016.06.042.

Tanong, K., Lan-Huong, T., Mercier, G., Blais, J.-F., 2017. Recovery of Zn (II), Mn (II), Cd (II) and Ni (II) from the unsorted spent batteries using solvent extraction, electrodeposition and precipitation methods. J. Clean. Prod. 148, 233–244. https://doi.org/10.1016/j.jclepro.2017.01.158.

Yesiltepe, S., Bugdayci, M., Yucel, O., Sesen, M.K., 2019. Recycling of alkaline batteries via a carbothermal reduction process. Batteries 5, 35. https://doi.org/10.3390/batteries5010035.